OPTOELECTRONICS AND ADVANCED MATERIALS – RAPID COMMUNICATIONS Vol. 1, No. 9, September 2007, p. 457 - 466

Far – field radiation characteristics in a dielectric environment

C. MERTZANIDIS*, L. MAGAFAS[a]
TEI of Kavala, Depart. of Industrial Informatics, 65404 Kavala, Greece
[a]TEI of Kavala, Depart. of Electrical Engineering, 65404 Kavala, Greece

The far - field characteristics of line sources lying between the slabs of a multi - dielectric substrate configuration are presented. Such a configuration is usual in the technology of microstrips as well as in remote sensing. The electric field is expressed in the form of a Fourier integral of the potential V(y,h), which is given by the solution of the 2-D wave equation. The unknown coefficients of the solution are found from the boundary conditions of the electric and magnetic fields at the interfaces of the substrates. A set of numerical results for one to many substrates media give interesting radiation patterns. The main conclusion is that the patterns from a line source are similar to that given in free space by a complex array of sources. Symmetric or non - symmetric configurations give patterns with the corresponding characteristics. The ray optical techniques fail for more than three substrates, due to multi - reflection and refraction, while our procedure can be applied for any set of lossless or lossy substrates.

Received August 7, 2007; August 25, 2007)

Keywords: Radiation patterns, Dielectrics, Signal processing, Remote sensing, Microstrip antennas

1. Introduction

Remote sensing, many microstrip antennas as well as other antenna arrays are all based on the reflection and refraction effects of multilayered dielectric structures. A lot of interesting studies are found in the international literature, where different theoretical models solve problems related with the above mentioned applications. A line source, that lies on the interface between two dielectric substrates, is one of the most attractive models. Many cases ([1] – [10]) have been given in the past, where in [9] the patterns of a line source lying in a medium with up to four substrates are presented. From the results of these studies it was found that many differences appear, due to the different number of the substrates as well as the different dielectric constants and thicknesses. Pattern maxima can be controlled by combining the geometrical and physical characteristics of the layers and show an interesting flexibility as the number of layers increases.

Following the solution of a four - dielectric substrate system we can see that the analytical process is very complicated. We must say that it is not possible - or, anyway, it is hardlaboured - to follow the same method if we increase the number of substrates to more than four. Our present study has to do with the investigation of the radiation from line sources lying in a multi - substrate medium. It seems that this is the more general case, which includes all the previous as specific ones. On the other hand, one can study radiation effects from linear arrays of point sources with any current distribution, which arrays are mounted into a dielectric structure.

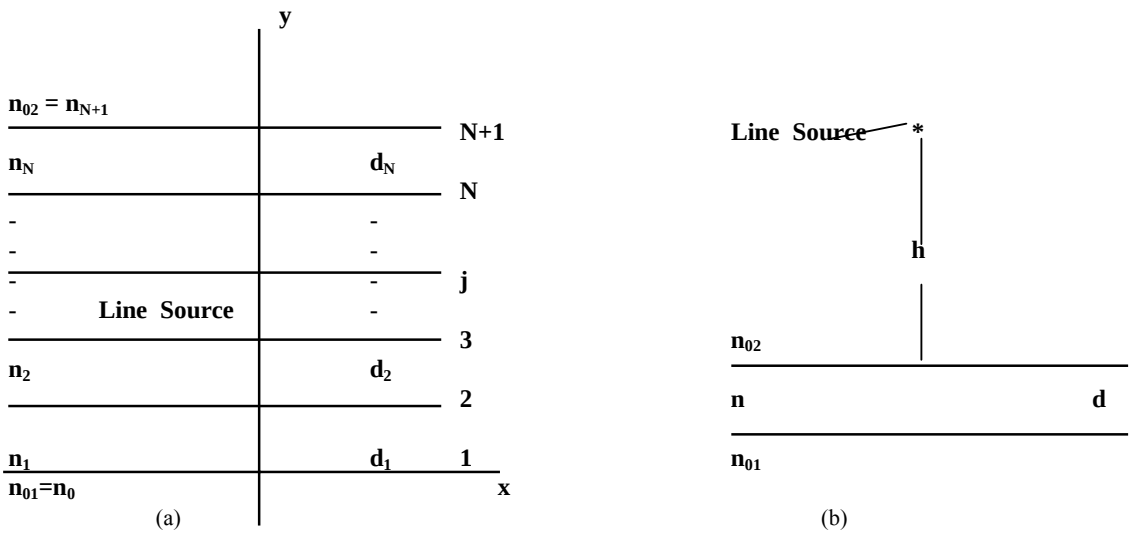

Fig. 1. (a)Geometry for the case of one source mounted between an N – layer dielectric structure .(b)Geometry of one dielectric slab and one source in distance h above the slab.

Fig. 1(a) shows our configuration geometry with a point source lying on the j – th interface. We can replace the point source by any linear array of sources, having the desired current distribution. The line sources can be put at any position into or outside the above mentioned configuration. On both sides of the system we have unbounded space, not necessary air. There is no quantitative limitation for n_i and d_i (i = 1, 2, . . . , N). It is possible to reduce the geometry by zeroing one or more substrate thicknesses. It must be pointed out, that our method is not limited. That happens because the whole procedure is not based on any analytical expression of the field but on a suitable numerical computation.

2. Formulation

For the geometry given in Fig. 1(a), the electric field is derived from the solution of the wave equation

$$\nabla^2 E_z + k^2 E_z = -j\omega\mu I\delta(x)\delta(y) \quad . \quad (1)$$

$$k^2 = \omega^2\mu\varepsilon \quad , \quad \varepsilon = n^2\varepsilon_o$$

(μ = permeability, ε = permittivity, n = index of refraction)

We can write the solution of (1) in the form of the Fourier integral given by

$$E_z(x,y) = \int_{-\infty}^{\infty} V(y,h)e^{jhx}dh \, . \quad (2)$$

By combining (1) and (2), we find that the potential V(y,h) satisfies the differential equation

$$\frac{d^2V_i}{dy^2} + (k_i^2 - h^2)V_i = -j\frac{\omega\mu_0}{2\pi}I_j\delta(y-y_j) \quad (3)$$

where

$$\delta(x) = \frac{1}{2\pi}\int_{-\infty}^{\infty} e^{ihx}dh \quad (4)$$

In (3) we have i = 0, 1, 2, . . , j, . . , (N+1) (for the unbounded space and the substrates),
$\delta(y-y_j)$ is the Dirac delta function,
I_j is the amplitude of the current of the line source, which is located at the j^{th} interface, and
V_i is the function, which for any of the subregions takes one of the following forms:

$$V_{01} = a_0 e^{\sqrt{h^2-k_{01}^2}\,y} \quad \text{for} \quad y < 0$$

$$V_{02} = b_0 e^{-\sqrt{h^2-k_{02}^2}\,y} \quad \text{for} \quad y > \sum_{i=1}^{N} d_i$$

$$V_i = a_i e^{\sqrt{h^2-k_i^2}\,y} + b_i e^{-\sqrt{h^2-k_i^2}\,y} \quad \text{for} \quad \sum_{j=1}^{i} d_j > y > \sum_{j=1}^{i-1} d_j \quad i=1,2,\ldots,N \quad (5)$$

The 2N+2 unknown coefficients a_i, b_i (i= 0, 1, 2, . . . , N) can be found from the boundary conditions at the interface of the substrates of our model. These conditions are:

$$V_{01} = V_1 \quad \text{for} \quad y = 0$$

$$V_N = V_{02} \quad \text{for} \quad y = \sum_{i=1}^{N} d_i \quad (6)$$

$$V_i = V_{i+1} \quad \text{for} \quad y = \sum_{j=1}^{i} d_j \quad i=1,2,\ldots,N-1$$

and

$$\left.\frac{dV_1}{dy}\right|_{y=\Delta y} - \left.\frac{dV_{01}}{dy}\right|_{y=-\Delta y} = -j\frac{\omega\mu_0}{2\pi}I_{01}\delta_{01,j}$$

$$\left.\frac{dV_i}{dy}\right|_{y=\sum_{j=1}^{i-1} d_j+\Delta y} - \left.\frac{dV_{i-1}}{dy}\right|_{y=\sum_{j=1}^{i-1} d_j-\Delta y} = -j\frac{\omega\mu_0}{2\pi}I_j\delta_{ij} \quad (i=2,3,\ldots,N)$$

$$\left.\frac{dV_{02}}{dy}\right|_{y=\sum_{i=1}^{N} d_i+\Delta y} - \left.\frac{dV_N}{dy}\right|_{y=\sum_{i=1}^{N} d_i-\Delta y} = -j\frac{\omega\mu_0}{2\pi}I_{02}\delta_{02,j} \quad (i=1,2,\ldots,N) \quad (7)$$

Eqs. (6) and (7) with the help of (5) form a linear system of 2N+2 equations with 2N+2 unknowns. From the unknowns we need only a_0 and b_0, because these are the only necessary coefficients for the derivation of the far field's expressions at $0^o \le \varphi \le 180^o$ and $180^o \le \varphi \le 360^o$ regions (outside the layered configuration).

To find the far field we use Eq. (2), where we apply the Stationary Phase Method, [12]. This method gives the asymptotic expansion of the integral (2).

For justification of the use of this method, let us see a generalized Fourier integral of the form

$$I(x) = \int_a^b f(t)e^{jx\psi(t)}dt \, , \quad (8)$$

where f(t), ψ(t), a, b, x and t are real. For $\psi(t) = t$, the above generalized Fourier integral is simply an ordinary Fourier integral. If for $a \le t \le b$ there is a t (a point), for which $\psi^{(n)}(t)\big|_{t=\alpha} = 0$, n = 1, 2, . . . , p-1 and $\psi^{(p)}(t)\big|_{t=\alpha} \neq 0$, then this point is called a *Stationary Point* of ψ(t). For $x \to \infty$, the asymptotic approximation of I(x) is given by

$$I(x) \underset{x\to\infty}{\approx} f(\alpha)e^{jx\psi(\alpha)\pm j\frac{\pi}{2p}}\left[\frac{p!}{x\left|\psi^{(p)}(\alpha)\right|}\right]^{1/p}\frac{\Gamma(1/p)}{p} \quad (9)$$

$e^{+j\frac{\pi}{2p}}$ is used when $\psi^{(p)}(\alpha) > 0$, while $e^{-j\frac{\pi}{2p}}$ is used when $\psi^{(p)}(\alpha) < 0$. We apply (9) in our case, for which f(t) is substituted by V(y,h). The electric field in the unbounded space becomes

$$E_{z01} = \int_{-\infty}^{\infty} a_0(h, k_i, d_i) e^{\sqrt{h^2 - k_{01}^2}\, y} e^{jhx} dh \quad (10)$$

$$E_{z02} = \int_{-\infty}^{\infty} b_0(h, k_i, d_i) e^{-\sqrt{h^2 - k_{02}^2}\, y} e^{ihx} dh \quad (11)$$

We transform the above eqs. (10) and (11) replacing x and y by

$x = \rho\cos\varphi$, $y = \rho\sin\varphi$

and also $h = n_{01}k_0\sin\varphi$ for (10)

$h = n_{02}k_0\sin\varphi$ for (11).

After this transformation, the integrals (10) and (11) take the form of (8), for which the asymptotic expression is given by (9). In our case ψ(t) corresponds to sin(α + φ) with independent variable α instead of t. The first derivative of ψ is equal to zero when α + φ = π/2. Eqs. (10) and (11) can be approximated by (9). So, for each angle φ we use (6) and (7) to find a_0 and b_0, for which the integrand expressions are calculated from (9) by setting p = 2. The radiation pattern is found from the time - averaged Poynting Vector S(φ),

$$S(\phi) = \frac{1}{2} n_{0i} \sqrt{\frac{\varepsilon_0}{\mu_0}} |E_{z0i}|^2 \quad , \quad i = 1, 2 \quad (12)$$

In Appendix we give, as an example, the form of the linear system for the derivation of the coefficients a_o and b_o for a case of 6 dielectric slabs. The total current I_i of all sources, just for computational convenience, is accompanied by a parameter m_i, which specifies the current distribution.

One can find analytical expressions for a_o and b_o, solving the linear system of equs. (6) and (7). In any case, this is a system of 2N+2 equations. Instead of finding these analytical expressions, we can use appropriate computer programs, by means of which we can avoid the derivation of complicated expressions. We checked the numerical method for cases up to 8 dielectric substrates and the results were in absolute coincidence with the analytical one.

3. Radiation pattern results

To confirm our numerical results we compared them with those corresponding to simpler cases studied in the past. The radiation patterns taken by the method we described above are in exact agreement with those presented in ([7] - [9]) as well as in [11] for any linear array and in [10] for microstrip antenna with a dielectric cover ([10], Fig. 3.14). We will present in this paragraph the radiation patterns for some other cases which are of practical interest.

We first give the patterns of a model with simple slabs covered by air. Fig. 1(b) shows the geometry of the one slab model. The line source is at a distance h above the slab. (This h is not the parameter h in the theoretical formulation above).

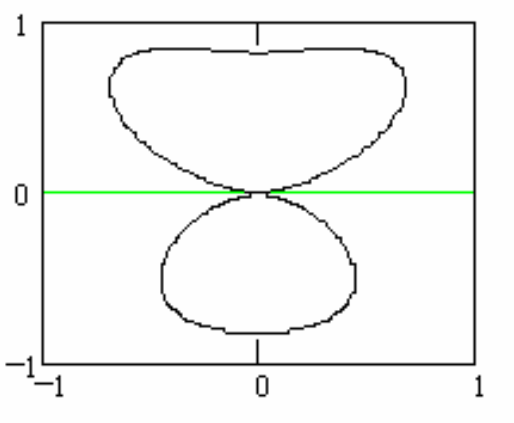

(a)

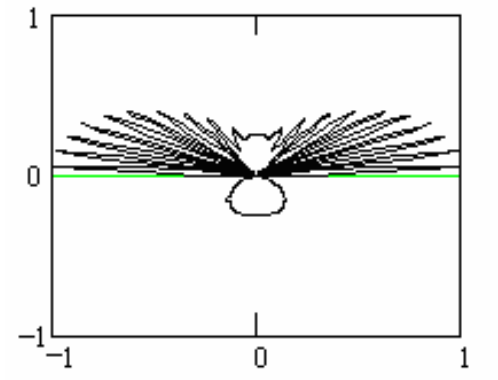

(b)

Fig. 2. Radiation patterns of a line source above a slab with d=0.5λ, n=8 at (a) h=0.05λ (b) h=5λ..

The radiation patterns of Fig. (2) correspond to the simple configuration of Fig. 1(b) with $n_{01} = n_{02} = 1$, n = 8, d = 0.5λ, h = 0.05λ (Fig. 2(a)) and h = 5λ (Fig. 2(b)). In the case of Fig. 2(a) we see, that the reflection and refraction effects inside the dielectric slab are not strong and we have two comparable lobes in both sides of the dielectric, with the main lobe being located at the side of the dielectric slab. In the case of Fig. 2(b), the reflection and refraction effects are strong, which result to this peculiar pattern with a lot of secondary lobes at the side of the slab.

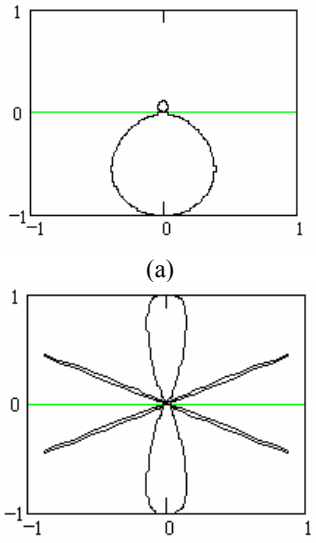

Fig. 3. Radiation patterns of a line source above a slab with (a) d=0.1λ, n=8 (b) d=10λ, n=8

The radiation patterns of Fig. 3 correspond to another simple case, where we have one line source mounted on a single slab and the unbounded space being air. Fig. 3(a) gives the case with the slab having n=8 and d=0.1λ. The main lobe is located at the side of the substrate with n=8. In Fig. 3(b) we increased d from 0.1λ to 10λ, keeping all the other parameters of the configuration invariant. One can see, that the radiation pattern presents an interesting symmetry with strong the effect of reflection and refraction inside the dielectric slab.

If the dielectric is considered lossy (e.g. n=8-j0.05), the characteristics of the pattern are different at all for the case of d=10λ, while for d=0.1λ the lossy dielectric doesn' t appear any important influence. (The patterns are not shown here).

A model with air caged between four dielectric slab configuration (Fig. 4(a)) is a case similar to that already studied with two instead of four slabs. Comparing our results with these of [9] we conclude that we have similar radiation patterns. These patterns are symmetric due to the symmetry of the geometry and the number of main lobes increases with the thickness of the air layer. Fig. 4(b) gives the pattern for a case of four slabs corresponding with the geometry of Fig. 4(a).

Considering lossy instead of ideal dielectrics, we saw that the radiation patterns for the configuration of Fig. 4(a) don' t have any significant difference, except that the secondary lobes disappear.

A six dielectric slab model with one or more line sources gives radiation patterns depending on the refraction index profile. A rule for the form and the maxima of the radiation patterns can not be extracted.

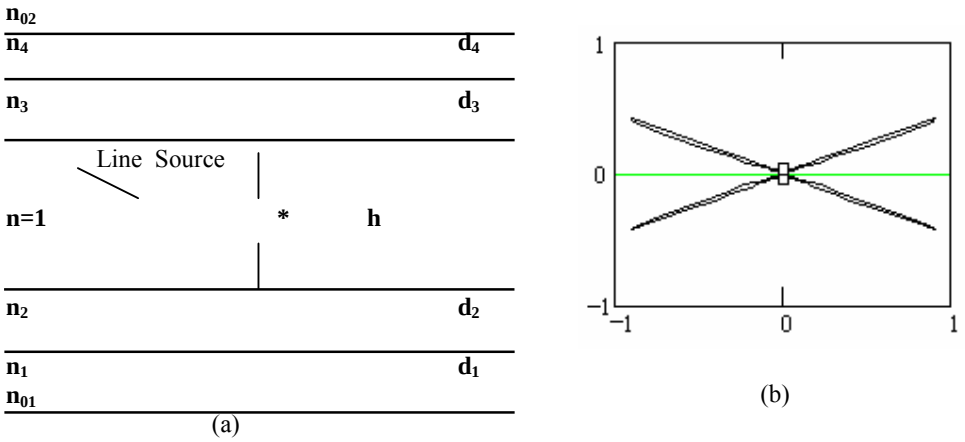

Fig. 4. (a) Air caged between four dielectric slabs model. (b) Radiation pattern of a line source lying into the above (a) model with h=1λ, $d_1 = d_2 = d_3 = d_4 = 0.25\lambda$, $n_1 = n_4 = 8$, $n_2 = n_3 = 4$.

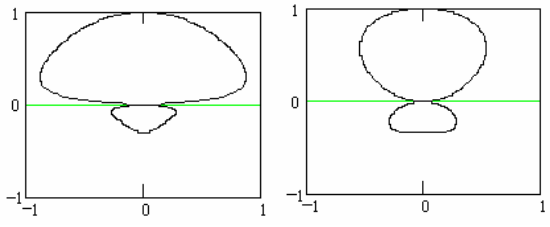

Fig. 5. Radiation patterns of line sources lying into a six slabs model with $n_{01}=n_{02}=1$, $d_i=0.1\lambda$, $n_{i+1} = n_i - 0.5$ (i=1,2,...,5). (a) One source at interface 2, $n_1=4$, (b) Two sources at interfaces 4 and 6, $n_1=4$.

Figs. 5(a) and (b) give the patterns for one and two line sources with $n_1 = 4$ and $n_{i+1} = n_i - 0.5$, i = 1, ... , 5 and $n_{01} = n_{02} = 1$. Both patterns show the maximum at the side of smaller n_i. In the same model, if we start from $n_1 = 7.5$ keeping the same rule for the index of the other slabs, we finally receive patterns (not shown here) with maxima at the opposite side of the previous case.

The above two profiles can be studied also for $n_{01} = n_{02} = 8$. In this case the main lobe appears at the side which is near to the line source. Figs. 6(a) and (b) give the radiation patterns for the geometries corresponding to Figs. 5(a) and (b).

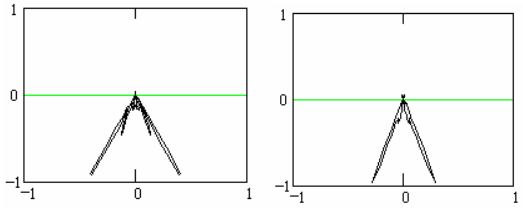

Fig. 6. Radiation patterns in correspondence with those of Fig. 5, but with $n_{01}=n_{02}=8$.

Another interesting model is that of Fig. 7(a), where we have a parabolic profile in the refraction index. For $n_{01} = n_{02} = 1$ we present two cases. The first has n = 3 and seven line sources and the other n = 9 and one line source. Fig. 7(b) for $d_i = 0.05\lambda$ and seven sources shows a symmetric pattern, which is similar to that of an array with line sources in distances in the free space more than $\lambda/2$. It is evident that our model gives the same results with the array in very small size. For one line source the pattern gives one lobe at the side of the source. Fig. 7(c) shows such a pattern, where the non - symmetric behaviour is evidenced.

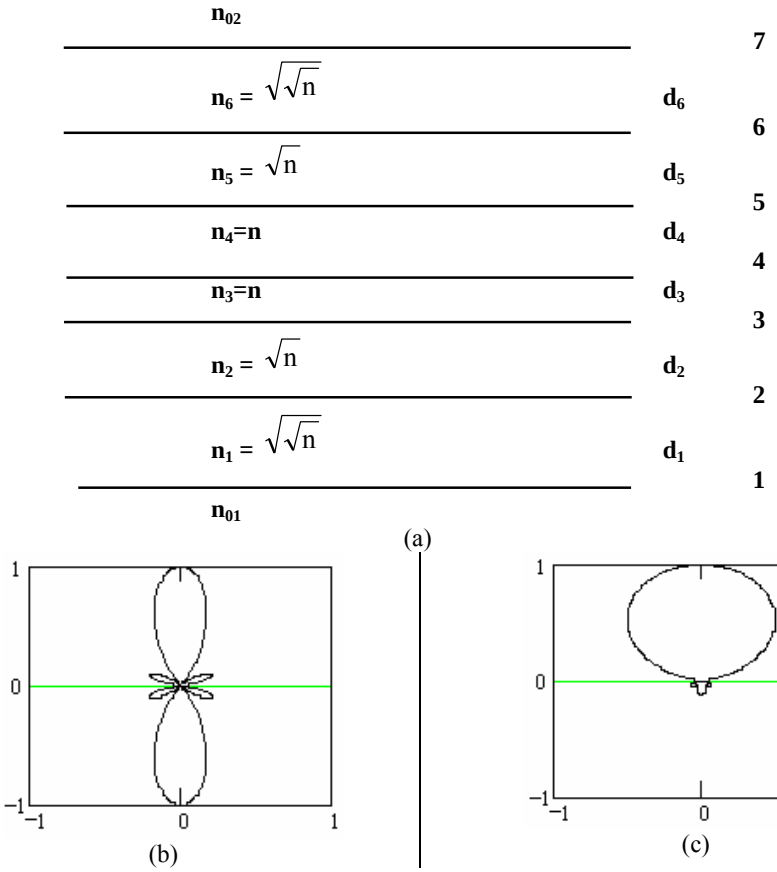

Fig. 7. (a) A model with parabolic profile in refraction indices.(b)Radiation pattern of seven sources lying into the model (a), one at every interface, n=3, $d_i=0.05\lambda$, with $n_{01}=n_{02}=1$. (c) Radiation pattern of one source at interface 1 of model (a), n=9, $d_i=0.1\lambda$, with $n_{01}=n_{02}=1$.

Fig. 8. Radiation patterns in correspondence with those of Fig. 7, but with $n_{01}=n_{02}=8$.

The radiation patterns for the above two cases but with $n_{01} = n_{02} = 8$ are shown in Figs. 8(a) and (b) respectively. Comparing these Figures with Figs. 7(b) and (c) we conclude that the unbounded space plays an important role.

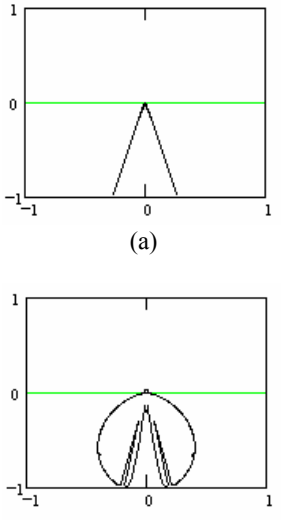

Fig. 9.Radiation patterns in correspondence with those of Figs.7 and 8, but with $n_{01}=8$, $n_{02}=1$.

This is more clear for $n_{01} = 8$ and $n_{02} = 1$, where it is expected to have the main lobe at the side of n_{01}. Figs. 9(a) and (b) give two patterns with the above behaviour.

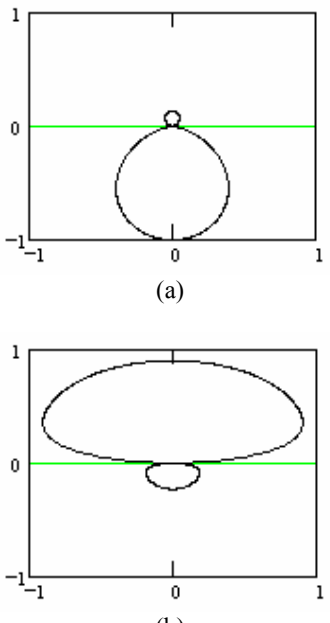

Fig.10.Radiation patterns of one line source lying into a six slabs model at the 7th interface, with $n_{01}=n_{02}=1$ and (a) $n_{i+1}=n_i+2$ (i=1,2,..,5, $n_1=2$),$n_id_i=0.05$ (b) $n_{i+1}=n_i-2$ (i=1,2,..,5, $n_1=12$), $n_id_i=0.1$

If we select a model with slabs of equal optical thickness (n_id_i = constant) for two different combinations of the refraction indices we have the patterns given in Figs. 10(a) and (b). The difference in the patterns shows that the optical length is one of the main characteristics of the medium.

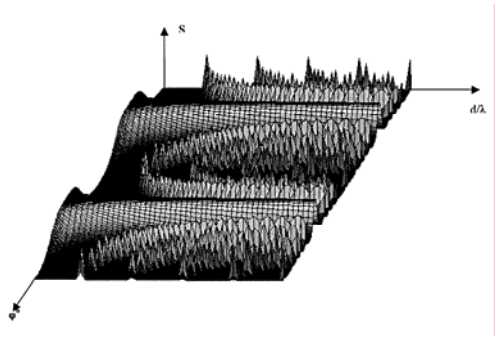

Fig.11. Radiation patterns of one source being located on a slab with n=10 and d varying from 0.5 λ up to 25 λ.

A last example studied by means of the above described method is that of Fig. 11. It is a very simple case, consisting of one dielectric slab with n=10, having air in both sides and one source being located on the top of the slab. The slab' s thickness varies from 0.5λ up to 25λ. The plot of Fig. 11 shows the evolution of the radiation pattern with increasing d. We see, that increase of d causes more and more secondary lobes, tending to disappear the nature of the main lobes.

All the examples given above could also be studied - theoretically - by the help of ray optical technique. This technique needs more complex description because of the multiple reflection and refraction through many slabs and it is almost impossible to be applied for a multislab medium. From the above given diagrams we understand that it is possible to achieve radiation patterns produced from one single line source similar to those taken by complex antenna arrays.

3. Conclusions

In this work the radiation patterns of one or more line sources lying on the interfaces of a multilayered medium are presented. The patterns are given by a numerical procedure, where the Stationary Phase Method is applied.

For the simple cases of one, two, three and four substrates our patterns were compared with those taken by analytical methods ([7] – [9]). Due to the degree of freedom in the choice of the profile of the medium and the position of the line sources, we were able to have more complex radiation patterns. The symmetry or non - symmetry in the profile produces the corresponding geometries in the radiation patterns.

The patterns have maxima and nulls in specific directions, which can be controlled by combining the characteristics of the model. The directional properties and the convenience to change the behaviour of the systems allows us to use them in remote sensing as well as in complex receiving systems.

5. Appendix

In this Appendix we give the form of the linear system for the derivation of the coefficients a_o and b_o in equs. (10) and (11). This system corresponds to a six slab model but it can be easily generalized for more slabs.

$$
\begin{array}{cccccccccccccc}
A_{1,1}a_o & & +A_{1,3}a_1 & +A_{1,4}b_1 & & & & & & & & & & =0 \\
 & & A_{2,3}a_1 & +A_{2,4}b_1 & +A_{2.5}a_2 & +A_{2,6}b_2 & & & & & & & & =0 \\
 & & & & A_{3,5}a_2 & +A_{3,6}b_2 & +A_{3,7}a_3 & +A_{3,8}b_3 & & & & & & =0 \\
 & & & & & & A_{4,7}a_3 & +A_{4,8}b_3 & +A_{4,9}a_4 & +A_{4,10}b_4 & & & & =0 \\
 & & & & & & & & A_{5,9}a_4 & +A_{5,10}b_4 & +A_{5,11}a_5 & +A_{5,12}b_5 & & =0 \\
 & & & & & & & & & & A_{6,11}a_5 & +A_{6,12}b_5 & +A_{6,13}a_6 & +A_{6,14}b_6 & =0 \\
 & A_{7,2}b_o & & & & & & & & & & & +A_{7,13}a_6 & +A_{7,14}b_6 & =0 \\
A_{8,1}a_o & & +A_{8,3}a_1 & +A_{8,4}b_1 & & & & & & & & & & & =I_1 \\
 & & A_{9,3}a_1 & +A_{9,4}b_1 & +A_{9,5}a_2 & +A_{9,6}b_2 & & & & & & & & & =I_2 \\
 & & & & A_{10,5}a_2 & +A_{10,6}b_2 & +A_{10,7}a_3 & +A_{10,8}b_3 & & & & & & & =I_3 \\
 & & & & & & A_{11,7}a_3 & +A_{11,8}b_3 & +A_{11,9}a_4 & +A_{11,10}b_4 & & & & & =I_4 \\
 & & & & & & & & A_{12,9}a_4 & +A_{12,10}b_4 & +A_{12,11}a_5 & +A_{12,12}b_5 & & & =I_5 \\
 & & & & & & & & & & A_{13,11}a_5 & +A_{13,12}b_5 & +A_{13,13}a_6 & +A_{13,14}b_6 & =I_6 \\
 & A_{14,2}b_o & & & & & & & & & & & +A_{14,13}a_6 & +A_{14,14}b_6 & =I_7
\end{array}
$$

Where:

$A_{1,1} = 1$ $A_{1,3} = -1$ $A_{1,4} = -1$

$A_{2,3} = e^{-\sqrt{h^2 - k_1^2}d_1}$ $A_{2,4} = e^{\sqrt{h^2 - k_1^2}d_1}$ $A_{2,5} = -e^{-\sqrt{h^2 - k_2^2}d_1}$ $A_{2,5} = -e^{\sqrt{h^2 - k_2^2}d_1}$

$A_{3,5} = e^{-\sqrt{h^2 - k_2^2}(d_1+d_2)}$ $A_{3,6} = e^{\sqrt{h^2 - k_2^2}(d_1+d_2)}$ $A_{3,7} = -e^{-\sqrt{h^2 - k_3^2}(d_1+d_2)}$ $A_{3,8} = -e^{\sqrt{h^2 - k_3^2}(d_1+d_2)}$

$A_{4,7} = e^{-\sqrt{h^2 - k_3^2}(d_1+d_2+d_3)}$ $A_{4,8} = e^{\sqrt{h^2 - k_3^2}(d_1+d_2+d_3)}$ $A_{4,9} = -e^{-\sqrt{h^2 - k_4^2}(d_1+d_2+d_3)}$ $A_{4,10} = -e^{\sqrt{h^2 - k_4^2}(d_1+d_2+d_3)}$

$A_{5,9} = e^{-\sqrt{h^2 - k_4^2}(d_1+d_2+d_3+d_4)}$ $A_{5,10} = e^{\sqrt{h^2 - k_4^2}(d_1+d_2+d_3+d_4)}$ $A_{5,11} = -e^{-\sqrt{h^2 - k_5^2}(d_1+d_2+d_3+d_4)}$ $A_{5,12} = -e^{\sqrt{h^2 - k_5^2}(d_1+d_2+d_3+d_4)}$

$A_{6,11} = e^{-\sqrt{h^2 - k_5^2}(d_1+d_2+d_3+d_4+d_5}$ $A_{6,12} = e^{\sqrt{h^2 - k_5^2}(d_1+d_2+d_3+d_4+d_5)}$ $A_{6,13} = -e^{-\sqrt{h^2 - k_6^2}(d_1+d_2+d_3+d_4+d_5)}$ $A_{6,14} = -e^{\sqrt{h^2 - k_6^2}(d_1+d_2+d_3+d_4+d_5)}$

$A_{7,2} = e^{-\sqrt{h^2 - k_{02}^2}(d_1+d_2+d_3+d_4+d_5+($ $A_{7,13} = -e^{-\sqrt{h^2 - k_6^2}(d_1+d_2+d_3+d_4+d_5+d_6)}$ $A_{7,14} = -e^{\sqrt{h^2 - k_6^2}(d_1+d_2+d_3+d_4+d_5+d_6)}$

$A_{8,1} = -\sqrt{h^2 - k_{01}^2}$ $A_{8,3} = -\sqrt{h^2 - k_1^2}$ $A_{8,4} = \sqrt{h^2 - k_1^2}$

$A_{9,3} = \sqrt{h^2 - k_1^2}e^{-\sqrt{h^2 - k_1^2}d_1}$ $A_{9,4} = -\sqrt{h^2 - k_1^2}e^{\sqrt{h^2 - k_1^2}d_1}$ $A_{9,5} = -\sqrt{h^2 - k_2^2}e^{-\sqrt{h^2 - k_2^2}d_1}$ $A_{9,6} = \sqrt{h^2 - k_2^2}e^{\sqrt{h^2 - k_2^2}d_1}$

$A_{10,5} = \sqrt{h^2 - k_2^2}e^{-\sqrt{h^2 - k_2^2}(d_1+d_2)}$ $A_{10,6} = -\sqrt{h^2 - k_2^2}e^{\sqrt{h^2 - k_2^2}(d_1+d_2)}$ $A_{10,7} = -\sqrt{h^2 - k_3^2}e^{-\sqrt{h^2 - k_3^2}(d_1+d_2)}$ $A_{10,8} = \sqrt{h^2 - k_3^2}e^{\sqrt{h^2 - k_3^2}(d_1+d_2)}$

$A_{11,7} = \sqrt{h^2 - k_3^2}e^{-\sqrt{h^2 - k_3^2}(d_1+d_2+}$ $A_{11,8} = -\sqrt{h^2 - k_3^2}e^{\sqrt{h^2 - k_3^2}(d_1+d_2+d_3)}$ $A_{11,9} = -\sqrt{h^2 - k_4^2}e^{-\sqrt{h^2 - k_4^2}(d_1+d_2+d_3)}$ $A_{11,10} = \sqrt{h^2 - k_4^2}e^{\sqrt{h^2 - k_4^2}(d_1+d_2+d_3)}$

$A_{12,9} = \sqrt{h^2 - k_4^2}e^{-\sqrt{h^2 - k_4^2}(d_1+d_2+d_3}$ $A_{12,10} = -\sqrt{h^2 - k_4^2}e^{\sqrt{h^2 - k_4^2}(d_1+d_2+d_3+d_4)}$ $A_{12,11} = -\sqrt{h^2 - k_5^2}e^{-\sqrt{h^2 - k_5^2}(d_1+d_2+d_3+d_4)}$ $A_{12,12} = \sqrt{h^2 - k_5^2}e^{\sqrt{h^2 - k_5^2}(d_1+d_2+d_3+d_4}$

$$A_{13,11} = \sqrt{h^2 - k_5^2}\, e^{-\sqrt{h^2 - k_5^2}(d_1 + d_2 + d_3 + d_4 + d_5)}$$

$$A_{13,12} = -\sqrt{h^2 - k_5^2}\, e^{\sqrt{h^2 - k_5^2}(d_1 + d_2 + d_3 + d_4 + d_5)}$$

$$A_{13,13} = -\sqrt{h^2 - k_6^2}\, e^{-\sqrt{h^2 - k_6^2}(d_1 + d_2 + d_3 + d_4 + d_5)}$$

$$A_{13,14} = \sqrt{h^2 - k_6^2}\, e^{\sqrt{h^2 - k_6^2}(d_1 + d_2 + d_3 + d_4 + d_5)}$$

$$A_{14,2} = -\sqrt{h^2 - k_{02}^2}\, e^{-\sqrt{h^2 - k_{02}^2}(d_1 + d_2 + d_3 + d_4 + d_5 + d_6)}$$

$$A_{14,13} = \sqrt{h^2 - k_6^2}\, e^{-\sqrt{h^2 - k_6^2}(d_1 + d_2 + d_3 + d_4 + d_5 + d_6)}$$

$$A_{14,14} = -\sqrt{h^2 - k_6^2}\, e^{-\sqrt{h^2 - k_6^2}(d_1 + d_2 + d_3 + d_4 + d_5 + d_6)}$$

$$I_1 = -j\frac{\omega\mu_o}{2\pi} Im_1 \qquad I_2 = -j\frac{\omega\mu_o}{2\pi} Im_2 \qquad I_3 = -j\frac{\omega\mu_o}{2\pi} Im_3 \qquad I_4 = -j\frac{\omega\mu_o}{2\pi} Im_4$$

$$I_5 = -j\frac{\omega\mu_o}{2\pi} Im_5 \qquad I_6 = -j\frac{\omega\mu_o}{2\pi} Im_6 \qquad I_7 = -j\frac{\omega\mu_o}{2\pi} Im_7$$

References

[1] D. Marcuse, ''Light Transmission Optics'', Van Nostrand - Reinhold, New York, 1972.
[2] D. Marcuse, ''Theory of Dielectric Optical Waveguides'', Academic Press Inc., New York, 1974.
[3] C. Elachi, C. Yeh, ''Mode Conversion in Periodically Disturbed Thin - Film Waveguides'', J. Appl. Phys. **45**, 3494 (1974).
[4] N. Engheta, C. H. Papas, C. Elachi, ''Interface Extinction and Subsurface Peaking of the Radiation Pattern of a Line Source'', Appl. Phys. **B26**, 231 (1981).
[5] R. W. P. King, G. S. Smith, ''Antennas in Matter'', M.I.T. Press, Cambridge, MA, 1981.
[6] O. S. Heavens, ''Optical Properties of Thin Solid Films'', Dover Publications Inc., New York, 1965.
[7] N. Engheta, C. Elachi, ''Radiation Characteristics of a Source in a Thin Substrate Mounted over a Dielectric Medium'', IEEE Trans. Antennas Propag., **AP - 36**(3), pp. 322 - 330, 1988.
[8] I. Diamandi, C. Mertzianidis, J. N. Sahalos, ''Radiation of a Line Source Mounted between Two Dielectric Substrates'', Can. J. Phys. **68**, 1486 (1990).
[9] I. Diamandi, C. Mertzianidis, J. N. Sahalos, ''Far – Field Patterns of Line Sources Mounted between Four - Dielectric Substrates'', Can. J. Phys., **70**, 173 (1992).
[10] V. W. Hansen, ''Numerical Solutions of Antennas in Layered Media'', J. Wiley & Sons, N.Y. (Research Studies Press LTD), 1989.
[11] W. L. Stutzman, G. A. Thiele, ''Antenna Theory and Design'', J. Wiley & Sons, N.Y. 1981.
[12] C. M. Bender, St. A. Orszag, ''Advanced Mathematical Methods for Scientists and Engineers'', McGraw - Hill Book Company, New York, 1978.

*Corresponding author: conmer@teikav.edu.gr